ELSEVIER

Polymer 42 (2001) 3799–3807

polymer

www.elsevier.nl/locate/polymer

Influence of crystal and amorphous phase morphology on hydrolytic degradation of PLLA subjected to different processing conditions

S. Iannace[a,*], A. Maffezzoli[b], G. Leo[c], L. Nicolais[a]

[a]*Department of Material and Production Engineering, Institute of Composite Material Technology, ITMC-CNR, University of Naples, Piazzale Tecchio 80, 80125 Naples, Italy*

[b]*Department of Innovation Engineering, University of Lecce, Via Monteroni, 73100 Lecce, Italy*

[c]*IME-CNR, Via Monteroni,73100 Lecce, Italy*

Received 23 March 2000; received in revised form 12 September 2000; accepted 10 October 2000

Abstract

Isothermal and non-isothermal crystallization kinetics of poly-L-lactide (PLLA) were studied in order to analyse the effect of crystalline and amorphous morphology on hydrolytic degradation. A modification of the nucleation/growing mechanism was observed in both isothermal and non-isothermal analysis. Samples isothermally crystallized at $T_c < 110$°C showed a higher fraction of amorphous phase which does not relax at T_g. Lower and decreasing values of this 'rigid-amorphous phase' fraction were detected at higher crystallization temperatures ($T_c > 110$°C). The effect of hydrolytic degradation on the amorphous and crystalline phases depends upon the initial morphology developed during the isothermal crystallization. The larger crystals developed at $T_c = 130$°C are more resistant to erosion compared to the less perfect and smaller crystals developed at higher levels of undercooling ($T_c = 90$°C). © 2001 Elsevier Science Ltd. All rights reserved.

Keywords: Poly-L-lactide; Crystallization; Hydrolysis

1. Introduction

The study of crystallization phenomena is of great importance in polymer processing for several reasons. The control of the temperature profile during cooling, in the final stage of a process, determines the development of a specific morphology which influences the final properties of the material. Cooling rate represents a key factor being responsible for the level of crystallinity and the crystal morphology. However, the modelling of non-isothermal crystallization implies a knowledge of kinetics and morphology developed at each isothermal crystallization temperature (T_c). Then, different morphologies can be obtained by changing the degree of undercooling operating either in isothermal conditions or in non-isothermal conditions using different cooling rates [1–4].

If crystallization is performed at high undercooling, the reduced molecular mobility enhances the nucleation rate as compared to the crystal growth rate, leading to the formation of a high number of smaller crystals. Depending on the molecular weight of the polymer, the number of interconnected chains between the crystals, and the number of chain segments, which are not regularly positioned in the crystal structure, can be modified. The molecular mobility of these amorphous regions is greatly reduced and they do not necessarily assume liquid-like mobility above the glass transition temperature [5–9]. The presence of amorphous immobilized chains affects the mechanical performance of the materials as well as their susceptibility to degradation.

In this work isothermal and non-isothermal crystallization of poly-L-lactide (PLLA) have been studied. Crystalline morphology and mobility of the amorphous phase were analysed as a function of crystallization temperature and cooling rate. The effects of crystallization conditions on hydrolytic degradation were then evaluated.

2. Materials and methods

The PLLA utilized in this work was purchased from Boheringer (Resomer® L214). Isothermal crystallization tests were performed in a temperature range of 90–135°C by Differential Scanning Calorimetry (DSC) using a Mettler DSC-30 and a Perkin–Elmer DSC-7. The samples were first melted for 2 min at 200°C, then cooled to the crystallization temperature at 50°C/min in order to

* Corresponding author.

E-mail addresses: iannace@unina.it (S. Iannace), maffez@axpmat.unile.it (A. Maffezzoli).

PII: S0032-3861(00)00744-8

analyse the crystallization kinetics as a function of T_c. The isothermally crystallized samples were characterized by thermal and dielectric analysis to correlate crystallization mechanisms to crystal morphology and molecular mobility of the amorphous phase. The procedures utilized for this analysis have been described in Refs. [10–11]. In order to analyse the effect of cooling rate on the development of crystalline morphology and the mobility of the amorphous phase, non-isothermal crystallization experiments were also performed.

Hydrolytic degradation was studied using films prepared by casting from a solution of chloroform; after the evaporation of the solvent, they were isothermally crystallized by a Mettler hot stage imposing the same thermal history employed in DSC analysis. They were degraded in a buffer solution at pH 7.02 for 40 weeks. Samples were periodically taken from the solution after 2, 4, 12 and 40 weeks, dried in a vacuum oven at 50°C overnight, and characterized by DSC, Wide Angle X-ray Diffractometry (WAXD) and Atomic Force Microscopy (AFM). WAXD has been performed using a standard instrument XRD-Philips equipped with a CuK_α source. The volume fraction of crystallinity calculated by WAXD has been estimated from the ratio of the integrated intensity of peaks associated with crystalline reflections and amorphous halo. Following this procedure the area proportional to the crystallinity fraction (A_c) is obtained by subtraction of the area under the amorphous halo from the total integrated area of the spectrum between $2\theta = 10°$ and $2\theta = 60°$ (A_{tot}). The volume fraction of crystallinity is then calculated as the ratio of A_c to $A_{tot.}$ [12]. AFM characterization of the films was carried out by a Topometrix Explorer Atomic Force Microscope operating in air in non-contact mode with a commercial low resonance frequency Si tip of 20 nm radius. Several scan sizes ranging from 50 μm × 50 μm down to 5 μm × 5 μm were recorded from different regions of the films to check the lateral uniformity of the morphology.

3. Results and discussion

3.1. Isothermal and non-isothermal crystallization

The Avrami equation, used to analyse the time dependence of the relative crystallinity, shows that the melt crystallization of PLLA can be described by a single Avrami exponent indicating that a single mechanism governs the entire process at each crystallization temperature T_c. This exponent is close to 3 for all the T_c investigated and this is an indication that the growing mechanism of crystals is three-dimensional and athermal [10]. Analysis of the half-time values $t_{1/2}$ indicates that the time taken to develop half of the crystallization is a strong function of T_c. Using a theoretical approach based on the Hoffman–Lauritzen theory [13], it can be shown that the linear growth rate G can be considered proportional to $1/t_{1/2}$ and therefore the temperature variation of $1/t_{1/2}$ can be written as:

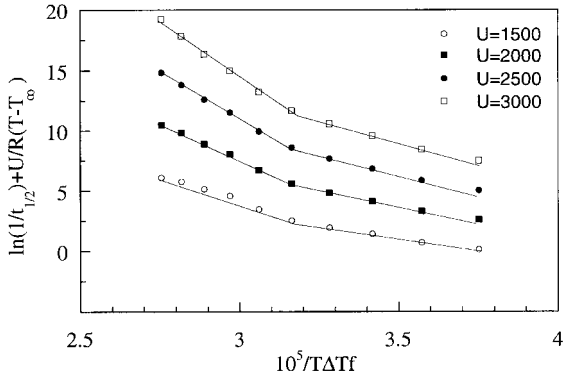

Fig. 1. Regime analysis. The slopes of the straight lines are related to the parameter K_g.

$$\left(\frac{1}{t_{1/2}}\right) = \left(\frac{1}{t_{1/2}}\right)_0 \exp\left[-\frac{U}{R(T_c - T_\infty)}\right] \exp\left[-\frac{K_g}{T_c \Delta T_f}\right] \quad (1)$$

where $T_\infty = T_g - 30$ K; $T_m^0 = 206$°C is the infinite-crystal melting point, evaluated by a Hoffmann–Week analysis; f is a correction term, which takes into account the change in heat of fusion with T_c; ΔT is the degree of undercooling; and U is the activation energy for segmental jump rate. K_g contains a constant integer number, n, whose value depends upon the crystallization regime. Hoffmann [14] recognized that the mechanism of crystallization from melts is a function of the degree of undercooling ΔT. Regime I, which usually occurs at low ΔT, is characterized by a growth rate G that is proportional to the surface nucleation rate i. At lower temperatures, multiple surface nuclei begin to occur on the substrate because of the rapid increase of i associated with the large undercooling and G become proportional to $i^{1/2}$, and the crystallization mechanism is indicated as regime II. Regime III is entered when the niche separation characteristic of the substrate in regime II approaches the width of a stem and, in these conditions, G is proportional to i.

In order to study the crystallization regimes in the temperature range investigated, experimental data were plotted as $\ln(1/t_{1/2}) + U/R(T_c - T_\infty)$ versus $1/T_c\Delta T_f$, according to the methods described by Hoffmann [14]. Several values of U were selected to analyse the results. The presence of two regions with different slopes (K_g), as reported in Fig. 1, is an indication that a transition from regime II to regime III (increase of K_g at higher undercooling) occurs around 115°C. This behaviour was observed for all the values given to the activation energy U.

Non-isothermal crystallization was performed in a range between 0.5 and 7°C/min. The degree of crystallinity decreased from 0.56 to 0.061 with an increase of cooling rate from 0.5 to 5°C/min. Crystallization performed at lower cooling rates (from 0.5 to 2°C/min) is accompanied by a

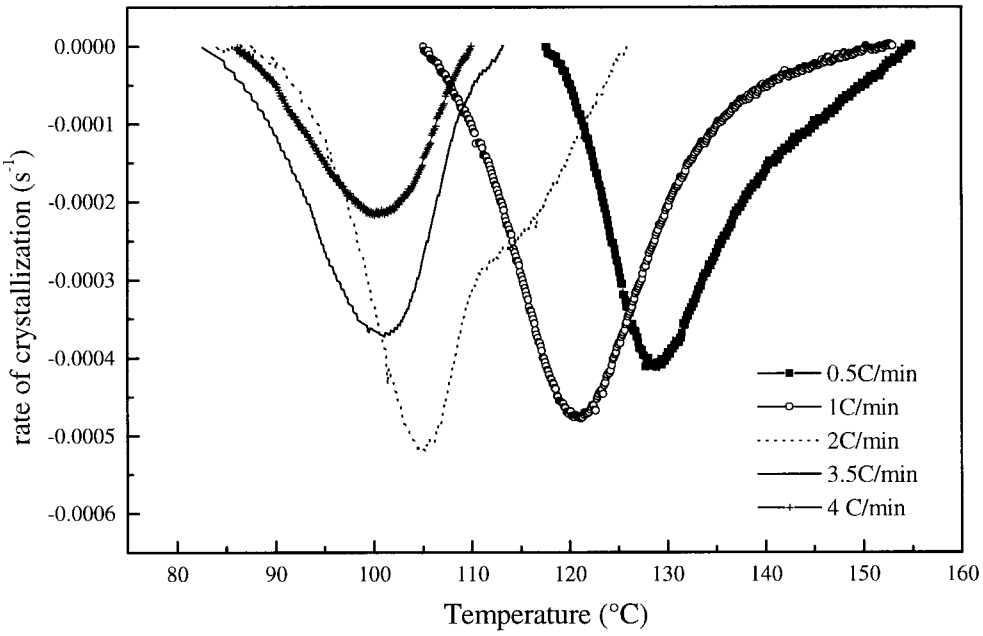

Fig. 2. Rates of crystallization obtained by DSC scan obtained at different cooling rates.

variation of the kinetics around 115°C (Fig. 2). In particular this is evident for the rate of crystallization evaluated at 2°C/min. This behaviour can be related to the transition from regime II to regime III occurring during the non-isothermal crystal growth, which leads to a heterogeneous crystalline morphology in the material. In Table 1 is reported the effect of cooling rate on some crystallization parameters and on the glass transition temperature of the amorphous phase.

Non-isothermal DSC data were processed to obtain a Continuous Cooling Transformation (CCT) plot, reported in Fig. 3 [15]. In this figure the iso-crystallinity curves are intersected by constant cooling rate curves. This plot may be considered as a fundamental tool for processing design indicating the development of morphology at different cooling rates. For cooling rates between 2 and 3.5°C/min the final crystallinity decreases to 0.1. For cooling rates higher than 5°C/min a fully amorphous polymer is obtained. Furthermore, the CCT plot indicates the processing conditions, in terms of cooling rates, that lead to crystal morphology corresponding to either regime II or regime III or to mixed morphologies.

Table 1
Effect of cooling rate: T_c is the crystallization temperature evaluated at the peak of the calorimetric curve; ΔH_c the enthalpy of crystallization; X_c the degree of crystallinity; and T_g the glass transition temperature

Cooling (°C/min)	T_c (°C)	ΔH_c (J/g)	X_c	T_g (°C)
0.5	128.4	44.4	0.56	65.7
1	121.2	40.2	0.51	66.5
2	104.6	24.3	0.46	65.5
3.5	101.2	8.5	0.10	62.6
4	100.2	6.0	0.076	61.7
5	99.1	4.9	0.061	61.1

3.2. Analysis of the amorphous phase

The glass transition temperature of PLLA, measured as the inflection point of the calorimetric curve, varies from about 71°C for $T_c = 90$°C to about 63°C for $T_c = 130$°C, and they are relatively higher compared to the amorphous polymer, which showed a T_g of about 62.5°C. The variation of T_g is usually explained by considering that the crystalline phase developed during the isothermal crystallization imposes constraints to the amorphous phase reducing the available configurations of the molecular chains that have, as a consequence, reduced mobility. The increase of T_g at a lower crystallization temperature is therefore an indication that the molecular mobility of the amorphous phase is reduced when the polymer is crystallized at a high level of undercooling. Thin lamellar crystals developed at high undercooling in regime III, characterized by irregular surfaces, impose a higher constraint on the mobility of the amorphous regions compared with those developed at low undercooling in regime II, characterized by thicker and more regular lamellae [12–14].

Crystallization performed under non-isothermal conditions also leads to materials with different glass transition temperatures. The amorphous phase of the PLLA displays a higher glass transition when the polymer is crystallized during slow cooling (Table 1). This is correlated to the high degree of crystallinity developed when the cooling rate is lower than 3.5°C/min. At higher cooling rates, samples crystallize predominantly under regime III, but the low degree of crystallinity developed does not affect the molecular mobility of the amorphous phase, as observed in isothermal crystallized samples.

The relaxation process which takes place at T_g can be

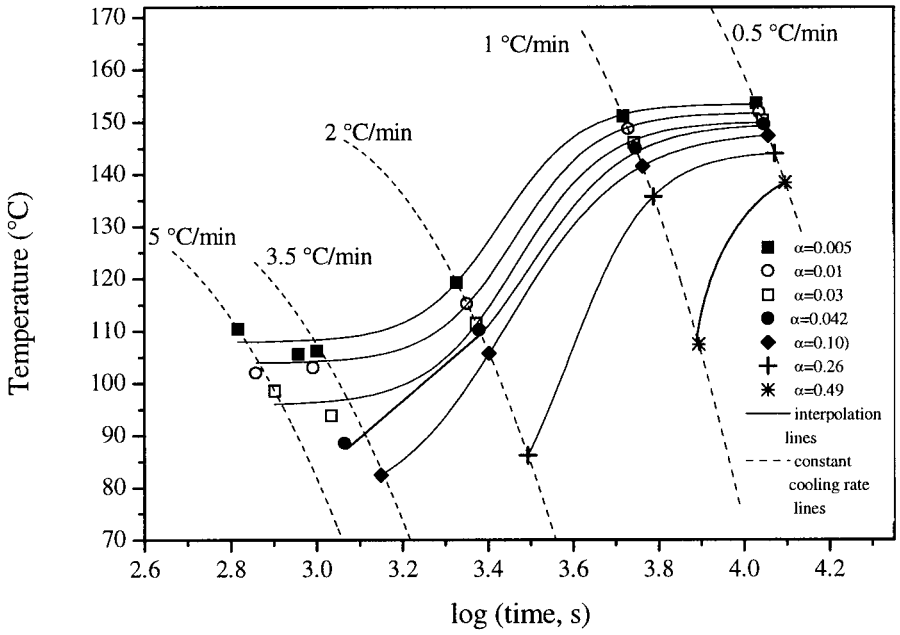

Fig. 3. CCT plot obtained from non-isothermal DSC data.

evaluated by measuring the increment of heat capacity $C_p(T)$ [8,9]. This increment is directly related to the fraction of the amorphous material that relaxes at T_g and therefore the change in the heat capacity is attributed only to the mobile amorphous fraction, which assumes liquid-like mobility within a narrow range of temperature around T_g. The difference between the liquid-like fraction and the rigid part of the amorphous phase is related to the different configurational entropy of the chains and this is reflected in the absence of a distinct heat-capacity change of the rigid amorphous phase at the glass transition step, where only the transition of the mobile amorphous fraction is observed.

The fraction of amorphous molecules that do not become liquid-like at T_g, the so-called rigid amorphous fraction (X_{raf}), can be therefore evaluated from the isothermal experiments by comparing the heat capacity increment of semi-crystalline and quenched amorphous materials at T_g, as specified in the following equations:

$$X_{raf} = \mathrm{fr} - X_c \tag{2}$$

$$\mathrm{fr} = 1 - \left[\frac{\Delta C_p(c)}{\Delta C_p(a)}\right] \tag{3}$$

where fr is the overall 'rigid fraction', $\Delta C_p(c)$ and $\Delta C_p(a)$ are the measured heat capacity increments at the T_g, respectively, for crystalline and amorphous samples. They were calculated by a linear extrapolation of the liquid heat capacity data above T_g and from solid heat capacity data below T_g. The degree of crystallinity X_c was measured from the isothermal heat of crystallization ΔH_c as follow:

$$X_c = \frac{\Delta H_c}{81} \tag{4}$$

where 81 J/g was used as the heat of fusion of the crystalline phase of PLLA [16,17]. This equation was checked on samples crystallized at $T_c = 120$°C and the degree of crystallinity, calculated with the two methods is quite similar (0.45 from DSC and 0.48 from X-ray). However, the effect of crystallization temperature on the heat of fusion of the crystalline phase was not analysed in this work and will be the topic of a future publication.

As shown in Fig. 4, the small variations of the total rigid fraction $\mathrm{fr} = X_{raf} + X_c$ indicates that the fraction of amorphous phase not relaxing at T_g is reduced by just 10% when the crystallization temperature is increased from 90 to 130°C. Since the crystallinity increases by more than 50% in the same range of temperature, it follows that a significant reduction of the rigid amorphous fraction X_{raf} occurs.

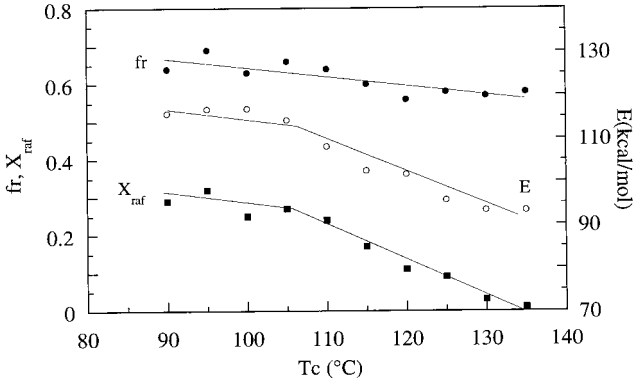

Fig. 4. Effect of crystallization temperature on molecular mobility. At higher T_c, under regime II conditions, the higher molecular mobility is related to lower values of X_{raf} and E.

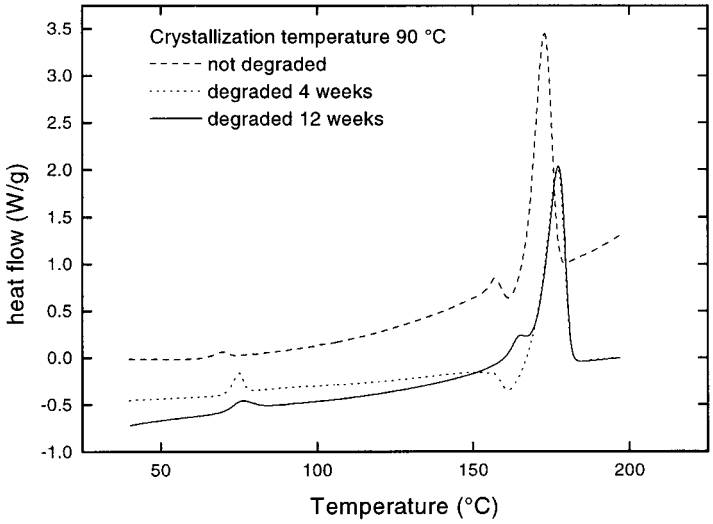

Fig. 5. Calorimetric scan of degraded PLLA. Sample were isothermally crystallized at 90°C.

Moreover, a correspondence between the slope variation of X_{raf} versus T_c and regime transition indicates that these two phenomena are correlated.

A powerful tool to examine the molecular mobility of polymeric chains is the analysis of the dielectric relaxation. The approach is based on the assumption that dipole relaxation depends upon the local environment and the response to an applied electric field is associated with local mobility. At a certain frequency and temperature, the number of dipoles that can respond to the electric field is therefore related to their ability to move. As an example, crystalline dipoles are more tightly bound in the environment then amorphous dipoles and thus they are not able to respond at certain frequencies. Equivalently, dipoles that are a part of the rigid amorphous phase have lower mobility and they respond differently than the 'liquid-like' amorphous molecules.

In our previous work we have shown that in the glass transition region, the temperature dependence of dielectric loss ϵ'' shows a well-defined peak whose intensity increases and shifts to higher temperature as the applied frequency increases [10]. The analysis of the chain stiffness against the segment motions can be performed by calculating the apparent energy of activation (E) of the relaxation process by means of the following Arrhenius' equation:

$$f = f_0 \exp\left(-\frac{\mathrm{E}}{\mathrm{R}T}\right) \tag{5}$$

where f is the applied frequency, T is the temperature corresponding to the maximum values of e'' and f_0 is the extrapolation of the frequency at $T = \infty$.

The activation energy, calculated from the above equation, is shown in Fig. 4 versus the crystallization temperature T_c. The decrease of E is in agreement with the results obtained from thermal analysis. The rigid amorphous fraction X_{raf} and the apparent activation energy show similar trends. Little variations were observed for T_c up to 105°C and this is followed by a progressive reduction of the immobilization effect in the amorphous phase. This is accompanied by a simultaneous decrease in the apparent activation energy E, which can be seen as the thermodynamic barrier to the molecular movement [18].

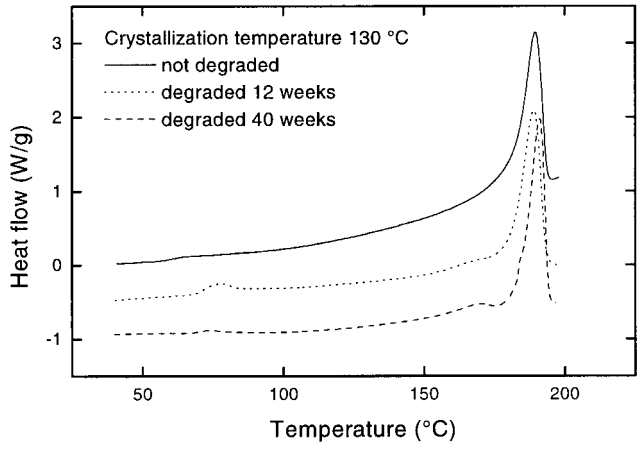

Fig. 6. Calorimetric scan of degraded PLLA. Sample were isothermally crystallized at 130°C.

3.3. Hydrolytic degradation

The effect of hydrolysis on the thermal properties of PLLA was evaluated by performing calorimetric scans on samples taken from the buffer solution and dried in a vacuum oven. Figs. 5 and 6 report the DSC heating scans on samples isothermally crystallized at 90 and 130°C before and after degradation and the calorimetric data are reported in Table 2.

At 90°C PLLA crystallizes under regime III and the morphology of the samples is characterized by a high

Table 2
Effect of crystallization temperature on transition temperatures (T_g and T_f) and on the degree of crystallinity during hydrolysis

T_c (°C)	Time (weeks)	T_g (°C)	T_f (°C)	X_c (X-ray)
90	0	71	180	0.46
	4	73	177	0.42
	12	73	177	0.41
	40	–	–	0.30
130	0	63	189	0.44
	4	71	192	0.44
	12	71	189	0.45
	40	71	191	0.54

number of small crystals with irregular fold surface, and a high fraction of rigid amorphous phase. The calorimetric behaviour of samples degraded for four weeks, shown in Fig. 5, is similar to the behaviour of undegraded materials. Samples crystallized under regime III are characterized by the presence of two peaks of fusion and the first of them is followed by a small exothermal event. The first endothermic peak is due to the fusion of crystals of lower dimension which, recrystallizing, give rise to the small exothermal event, as observed also by other authors for polylactides [19].

Thin and irregular lamellar crystals, grown under regime III, are the consequence of the presence of quite short effective substrate length arising from the proximity of the niches and this implies that molecules crystallize in the form of small sets of stems on the rough growth front [14]. Therefore, due to the abundance of closely spaced niches, adjacent re-entry is not favoured and the crystal morphology is not characterized by regular chain folding. Then, both the degree of perfection of the crystals and the maximum crystallinity achievable are affected.

The recrystallization peak is less evident in samples degraded for 12 weeks. Another small endothermic peak appear at $T_f^1 = 164.4$°C (Fig. 5), lower than the main peak at $T_f = 180$°C, due to the fusion of the smaller and less perfect crystals. After isothermal crystallization, this portion of crystalline phase is characterized by a high number of fragments of amorphous chains (the rigid amorphous phase) and interconnecting portions of crystals which are characterized by a high surface energy, due to the irregularity of the fold surface. These fragments are broken during the hydrolysis and this leads to a reduction of the crystalline surface free energy. As a consequence, the melting temperature of the crystals increases while the tendency towards the recystallization phenomena, which are favoured by the excess of surface free energy present in the imperfect crystals developed under regime III, is reduced. Moreover, as discussed below, the degradation of the amorphous phase favours the erosion of the crystalline phase, and for this reason melting-recrystallization phenomena observed in the undegraded samples become negligible.

The crystalline phase of PLLA, isothermally crystallized at 130°C (Fig. 6) under regime II, is characterized by higher temperature of fusion ($T_f = 189$°C) due to the greater dimension of the crystals. They do not show the double peak previously discussed, and this confirms the presence of well-developed crystals. In these samples, hydrolytic degradation does not substantially affect the melting temperature, but it induces a slight increase in T_g. At 12 weeks of degradation, the endothermic peak around 168°C is very small compared to that shown in Fig. 5. This peak, as in the former case, is attributed to the melting of crystallites made of those degraded chain segments which are too long to diffuse into the buffer solution. These crystals may grow at low temperature during the DSC heating scan and not during the hydrolysis of the PLLA samples in the buffer solution at 37°C. At this temperature, PLLA is in the glassy state and the molecular mobility is very low. Under this condition, the crystallization process is not kinetically favoured and for this reason the presence of these crystals is probably correlated to the crystallization occurring during the heating scan. In this case, the smaller melting peak indicates that a slower degradation of the amorphous phase occurs in comparison with the samples crystallized at 90°C.

The main difference observed during the degradation of the two sets of PLLA samples regards the degree of crystallinity X_c, which was measured from X-ray spectra following the classical procedure described by Wunderlich [20] (see Table 2). Polymers crystallized at the higher level of undercooling (90°C) show a decreasing trend of X_c. Degradation advances in both the crystalline and amorphous regions, resulting in an overall decrease of the degree of crystallinity.

X_c of samples crystallized at higher T_c (130°C) always increases with the time of degradation. In this case, the hydrolysis of the amorphous phase and the loss of molecular fragments from the samples leads to an increase of the crystalline/amorphous ratio since the more perfect and stable crystals developed during the isothermal crystallization are hard to erode.

Figs. 5 and 6 are also characterized, in correspondance of T_g, by structural relaxation peaks of different intensities depending on the degradation time. In both cases the relaxation peak appears only after degradation in the buffer solution at 37°C. This may be explained as a classical ageing process in the glassy state during which the enthalpy and specific volume reduce, moving toward equilibrium and leading to a limited molecular mobility with an associated increase of the relaxation time of the amorphous phase of the polymer. However, at longer degradation times, the relaxation peaks become weaker due to a lower content of amorphous phase and probably also to a decrease of the characteristic relaxation time as a consequence of a significant reduction of the molecular weight. This inversion of intensities of the relaxation peaks occurs at four weeks for the sample crystallized at 90°C and at 12 weeks for the sample crystallized at 130°C. This result indicates that the crystalline morphology, developed at

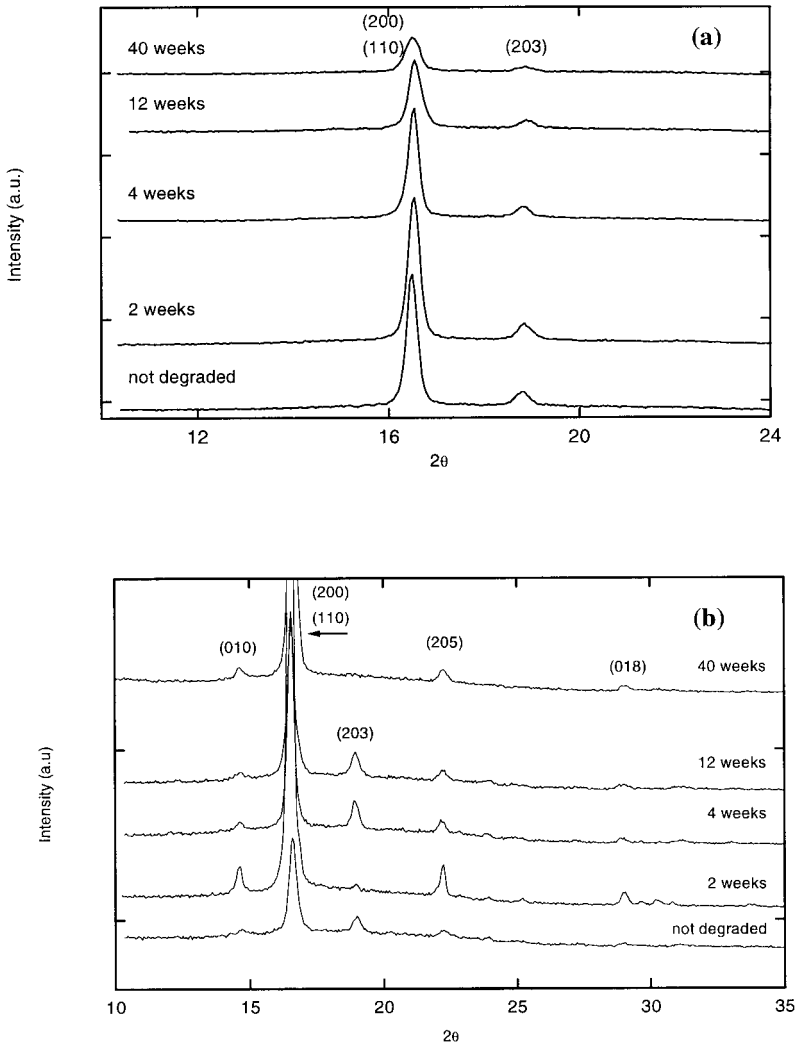

Fig. 7. WAXD data for sample crystallized at: (a) 90°C; and (b) 130°C at different times of hydrolysis.

different crystallization temperatures, affects the degradation kinetics of the amorphous phase and, as a consequence, the kinetics of the relaxation phenomena occurring at T_g.

X-ray analysis and morphological analysis by atomic force microscope, confirm these different mechanisms of degradation. The WAXD data, reported in Fig. 7a and b for the samples crystallized at 90 and 130°C show significant differences related to the crystallization temperature. In both cases the two main diffraction peaks, associated with the Miller indices (200) and (110) for the stronger peak and (203) for the weaker peak are observed always at the same angle [21]. Diffraction spectra obtained for the sample crystallized at 130°C are characterized by an increase of the

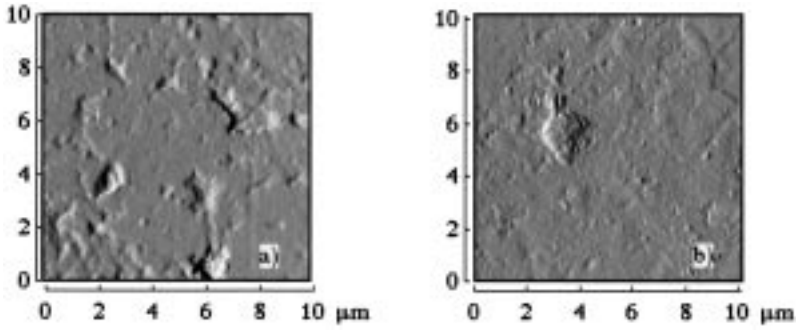

Fig. 8. AFM images of samples crystallized at: (a) 90°C before hydrolysis; and (b) and after 12 weeks of hydrolysis.

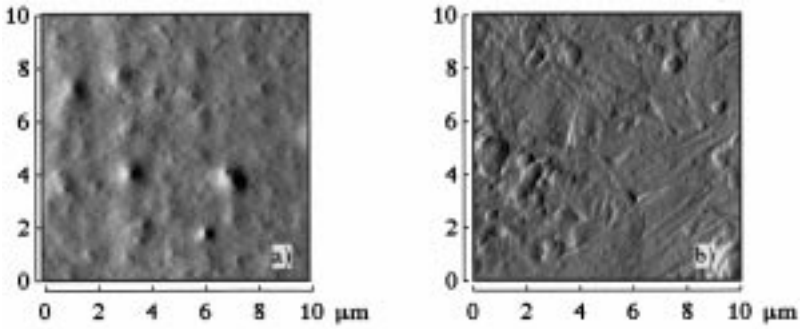

Fig. 9. AFM images of samples crystallized at: (a) 130°C before hydrolysis; and (b) and after 12 weeks of hydrolysis.

number of peaks up to 12 weeks followed by a decrease at 40 weeks. The degree of crystallinity continuously increases. As discussed, this behaviour may be the consequence of the improved hydrolytic stability of the crystalline phase developed in regime II at 130°C. In this case, the degraded amorphous phase may also originate new crystals (at 37°C, the local mobility can be enhanced by low molecular weight fragments), as well as the loss of low molecular weight fractions resulting in an increase of the degree of crystallinity.

The AFM images obtained on degraded and not degraded samples are reported in Figs. 8 and 9 for samples crystallized at 90 and 130°C, respectively. The surface morphology of the sample crystallized at 90°C is essentially unaffected by the degradation process (Fig. 8). Only a moderate increase of the root mean squared (RMS) roughness, from 7.00 to 9.70 nm is observed. On the other hand, the morphology of the sample crystallized at 130°C and degraded for 12 weeks is characterized by a newly formed rib-like asperities (Fig. 9), and by a RMS roughness increase from an average of 4.89 to 13.65 nm after degradation. In the first case the poor perfection of the crystals suggests a quasi-uniform degradation of both the amorphous and crystalline phases. In the second case the increased roughness and the new surface morphology may be associated to the selective degradation of the amorphous phase accompanied by the appearance of portions of the crystalline phase.

4. Conclusions

Isothermal crystallization kinetics of PLLA were studied as a function of the degree of undercooling. The crystallization rate shows a maximum around 105°C. Regime analysis allowed the detection of II → III transition around 115°C.

Analysis of the heat capacity increment at T_g of semicrystalline PLLA indicates the presence of an amorphous fraction which does not relax at T_g. Higher amounts of this rigid-amorphous phase were observed for $T_c < 110$°C. Lower and decreasing values were detected for T_c above 110°C, where crystallization occurs under regime II. Analysis of the activation energy of the relaxation behaviour, performed by dielectric experiments, confirms the variation of the molecular mobility of the amorphous phase with T_c.

The effect of hydrolytic degradation on the amorphous and crystalline phase depends upon the initial morphology developed during the isothermal crystallization. The larger crystals developed at higher T_c, under regime II, are more resistant to erosion compared to the less perfect and smaller crystals developed at higher levels of undercooling. The analysis of degradation is also supported from morphology indications obtained using AFM.

The analysis of non-isothermal crystallization indicated that the crystallization process changes during cooling from regime II to regime III at around 115°C. Moreover, the cooling rate affects the nucleation mechanism, the final degree of crystallinity and the morphology of the crystals. CCT curves were presented as a synthesis of the non-isothermal crystallization behaviour. An analysis of CCT curves shows a critical cooling rate of 5°C/min and allows the determination of the amount of crystalline phase growth in different regimes.

The morphology development originating from the processing conditions is strictly related with the hydrolytic degradation. The combination of the CCT curves and the data obtained from hydrolytic degradation may be considered as a basis for tailoring the morphology of the material to allow control of the rate of degradation during hydrolysis.

Acknowledgements

Dr F. Felline and Mr D. Cannoletta are gratefully acknowledged for DSC and X-ray measurements.

References

[1] Maffezzoli A, Kenny JM, Nicolais L. J Mater Sci 1993;28:4994.
[2] Lemstra PJ, Postma J, Challa G. Polymer 1974;15:757.
[3] Vilanova PC, Ribas SM, Guzman GM. Polymer 1985;26:423–8.
[4] Elyashevich GK, Poddubny VI. J Macromol Sci B: Phys 1990;29:249.
[5] Coburn JC, Boyd RH. Macromolecules 1986;19:2238.
[6] Plesu R, Malik TM, Prud'homme RE. Polymer 1992;33:4463.

[7] Suzuki H, Grebowicz J, Wunderlich B. Makromol Chem 1985;186:1109.
[8] Cheng SZD, Lim S, Judovits LH, Wunderlich B. Polymer 1987;28:10.
[9] Cheng SZD, Wu ZQ, Wunderlich B. Macromolecules 1987;20:2802.
[10] Iannace S, Nicolais L. J Appl Polym Sci 1997;64:911.
[11] Iannace S, Ambrosio L, Nicolais L. In: Ottembrite RM, editor. Frontiers in biomedical polymer applications, vol. 1. Lancaster: Technomic, 1998. p. 287–96.
[12] Wunderlich B. Macromolecular physics, vol. 1. New York: Academic Press, 1976.
[13] Hoffman JD, Davis GT, Lauritzen JI. Treatise on solid state chemistry: crystalline and non-crystalline solids. New York: Plenum Press, 1976.
[14] Hoffman JD. Polymer 1983;24:3.
[15] Torre L, Maffezzoli A, Kenny JM. J Appl Polym Sci 1995;56:985.
[16] Iannace S, Ambrosio L, Huang SJ, Nicolais L. J Appl Polym Sci 1994;54:1525.
[17] Fischer EW, Sterzel HJ, Wegner G. Kolloid-Zu Z Polim 1973;251:980.
[18] McCrum NG, Read BE, Williams G. Anelastic and dielectric effects in polymeric solids. New York: Wiley, 1967.
[19] Sarasua JR, Prud'homme RE, Wisniewski M, Le Borgne A, Spassky N. Macromolecules 1998;31:3895.
[20] Wunderlich B. Macromolecular physics, vol. 2. New York: Academic Press, 1976.
[21] Miyata T, Masuko T. Polymer 1997;38:4003.